0026-895X/94/010136-06$03.00/0

MOLECULAR PHARMACOLOGY, 45:136-141

Active and Inactive Enantiomers of 2β-Carbomethoxy-3β-(4-iodophenyl)tropane: Comparison Using Homogenate Binding and Single Photon Emission Computed Tomographic Imaging

B. E. SCANLEY, R. M. BALDWIN, M. LARUELLE, M. S. AL-TIKRITI, Y. ZEA-PONCE, S. ZOGHBI, S. S. GIDDINGS, D. S. CHARNEY, P. B. HOFFER, S. WANG, Y. GAO, J. L. NEUMEYER, and R. B. INNIS

Departments of Psychiatry and Diagnostic Radiology, Yale University School of Medicine and Veterans Affairs Medical Center, West Haven, Connecticut (B.E.S., R.M.B., M.L., M.S.A.-T., Y.Z.-P., S.Z., S.S.G., D.S.C., P.B.H., R.B.I.), and Research Biochemicals International, Natick, Massachusetts (S.W., Y.G., J.L.N.)

Received August 30, 1993; Accepted October 20, 1993

SUMMARY

2β-Carbomethoxy-3β-(4-iodophenyl)tropane (β-CIT; also designated RTI-55) is an analog of cocaine that has been developed as a single photon emission computed tomography radiotracer that labels dopamine and serotonin transporters. We have prepared the ^{125}I- and ^{123}I-labeled ([1*R*] "active" and [1*S*] "inactive") enantiomers of β-CIT. Total homogenate binding of the ^{125}I-labeled inactive isomer to baboon caudate and cortex was approximately equal to nonspecific binding of the active isomer in cortex and much lower than total binding of the active isomer in caudate. However, inactive isomer homogenate binding in caudate was somewhat higher than in cortex, and during single photon emission computed tomography scanning *in vivo* striatal (1*S*)-[^{123}I]β-CIT uptake was also slightly greater than in cortex. Following intravenous administration of the ^{123}I-labeled enantiomers, the plasma clearances of the active and inactive enantiomers were not significantly different. Single photon emission computed tomography imaging demonstrated that a bolus dose of nonradioactive (1*R*)-β-CIT rapidly displaced the uptake of (1*R*)-[^{123}I]β-CIT. In contrast, the brain uptake of (1*S*)-[^{123}I]β-CIT was not displaced by nonradioactive (1*R*)-β-CIT using either a bolus ("kinetic") or bolus plus constant infusion ("equilibrium") paradigm for administration of the radiotracer. In scans with bolus administration of radiotracer, peak striatal uptake of the active isomer was approximately twice that of the inactive isomer. In comparison to the ^{123}I-labeled active tracer, the inactive tracer showed earlier times to peak activity and faster washouts of activity in all brain regions. These studies demonstrate β-CIT stereoselectivity using both homogenate binding and *in vivo* imaging and suggest that the inactive enantiomer may be a useful measure of the kinetics of both blood-brain barrier transport and nonspecific binding.

[^{123}I]β-CIT is a radiolabeled analog of cocaine that has been developed as a SPECT radiotracer of monoamine transporters in the brain. β-CIT was developed from a family of cocaine analogs in which the phenyl moiety is attached directly to the tropane ring (*i.e.*, the ester bond is removed; 1). Madras *et al.* (2) reported that the fluorinated phenyltropane congener methyl 2β-(4-fluorophenyl)tropane-3β-carboxylate (CFT; WIN 35,428) had a higher affinity to DA transporters than cocaine itself. The iodinated analog of CFT was synthesized by both Boja *et al.* (3), who referred to it as RTI-55, and Neumeyer *et al.* (4), who referred to it as β-CIT. Subsequently, *in vivo* SPECT studies using (1*R*)-[^{123}I]β-CIT in baboons (5) have demonstrated high striatal uptake with very slow washout and a high striatal to occipital activity ratio. Following intravenous administration of [^{123}I]β-CIT, the vast majority of striatal activity represents binding to DA transporters, and midbrain activity primarily represents binding to 5-HT transporters (4, 5). Striatal activity was displaceable by GBR 12909, a selective DA uptake inhibitor, but not by citalopram, a 5-HT uptake inhibitor. In contrast, midbrain activity was displaced by citalopram but not by GBR 12909 (5).

Methods for *in vivo* quantification of these transporters are important because changes in DA and 5-HT transporters may be associated with several neuropsychiatric disorders. The euphoric and addictive effects of cocaine have been postulated to occur via cocaine's inhibition of the DA transporter (6), and the antidepressant bupropion may have its effect by inhibition of the DA transporter (7). Striatal DA transporters are decreased in Parkinson's disease and reflect the loss of DA terminal innervation (8, 9). A recent clinical SPECT study with (1*R*)-[^{123}I]β-CIT showed that patients with idiopathic

This work was supported by funds from the Department of Veterans Affairs (VA Schizophrenia Research Center and Substance Abuse Fellowship to B.E.S.), the National Parkinson Foundation, and NIMH (R43-MH48243).

ABBREVIATIONS: β-CIT, 2β-carbomethoxy-3β-(4-iodophenyl)tropane; DA, dopamine; 5-HT, serotonin; SPECT, single photon emission computed tomography.

Parkinson's disease had markedly decreased striatal uptake in comparison to age-matched healthy subjects (10).

Quantification of receptors with *in vivo* neuroimaging is complicated by the fact that the observed signal reflects not only specific receptor binding but also nonspecifically bound and free ligand and radiolabeled metabolites. Furthermore, several ligands have been shown to have regional differences in nonspecific binding and noninstantaneous, nonspecific binding kinetics (11–15). Theoretically, an inactive enantiomer would have physicochemical properties identical to those of the active compound except for the absence of specific binding. If enantioselectivity for the target site is demonstrated both *in vivo* and *in vitro*, then the radiolabeled inactive enantiomer may be used to quantify the kinetics of nonspecific binding and to define the rates of transport across the blood-brain barrier. Parameters derived from modeling of the inactive compound can then be used to improve the accuracy of modeling data acquired with the active isomer.

Similar to cocaine, β-CIT has four asymmetric centers and, therefore, 8 possible stereoisomers. The (*1R,2S,3S*) configuration (*i.e.*, the 2β,3β-substituted tropane moiety) gives the structure which we designate (1*R*)-β-CIT ("active isomer"). The (*1S,2R,3R*) configuration is designated (1*S*)-β-CIT ("inactive isomer"). The (1*R*)- and (1*S*)-isomers of β-CIT correspond to (−)- and (+)-cocaine respectively (see Fig. 1). When we refer to β-CIT without qualification, the active isomer (1*R*)-β-CIT is implied. All our previous studies have used the active isomer (1*R*)-β-CIT and not the racemic mixture. Wang *et al.* (16) have reported the synthesis of (1*R*)- and (1*S*)-β-CIT and have shown that (1*S*)-β-CIT has a 14,000-fold lower potency than (1*R*)-β-CIT for displacing (1*R*)-[^{125}I]β-CIT binding to rat striatal membranes. We now report the ^{125}I- and ^{123}I-labeling of (1*S*)-β-CIT and compare the binding properties of these enantiomers using *in vitro* brain tissue homogenates and *in vivo* SPECT imaging in baboons.

Materials and Methods

Radiolabeling. (1*R*)- and (1*S*)-[^{125}I]β-CIT and (1*R*)- and (1*S*)-[^{123}I]β-CIT were prepared as described previously (17) by no-carrier-added radioiodination of the trimethylstannyl precursor as reported by Neumeyer *et al.* (4) and Wang *et al.* (16). Purity was measured by high performance liquid chromatography and was >95%. Specific activity was measured by comparing UV absorbance of the labeled product with a standard curve made from known concentrations of nonradioactive β-CIT. The specific activity of the ^{125}I-labeled tracers was close to the theoretical maximum of 2200 Ci/mmol. Reagents were purchased from Sigma Chemical Co., St. Louis, MO, and used without further purification.

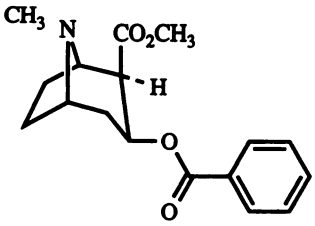

(−)-Cocaine

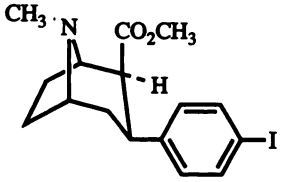

(*1R*)-ß-CIT

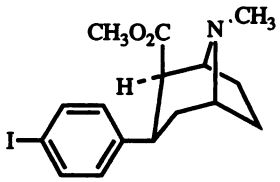

(*1S*)-ß-CIT

Fig. 1. Chemical structures of (1*R*)- and (1*S*)-β-CIT compared with the naturally occurring (−)-cocaine.

Homogenate binding. Tissue from two baboons (ovariectomized, female *Papio anubis*, 10–12 kg) was dissected immediately after death and frozen at −70°. On the morning of the assay, caudate nucleus and cortical tissues (including frontal, parietal, and occipital cortices) were thawed, weighed, and homogenized with a Polytron (setting 6 for 10 sec) in 1/40 (w/v) of artificial CSF buffer (128 mM NaCl, 3 mM KCl, 1.25 mM $NaH_2PO_4 \cdot H_2O$, 10 mM D-glucose, 2 mM $CaCl_2$, 2 mM $MgSO_4$, and 15 mM $NaHCO_3$, pH 7.4, at 22°). Tissue homogenates were centrifuged at 27,000 × *g* for 10 min at 4° and pellets were resuspended in buffer. This procedure was then repeated twice.

Incubation was initiated by the successive addition of 100 μl of (1*R*)- or (1*S*)-[^{125}I]β-CIT, 100 μl of buffer or nonradioactive compound, followed by 800 μl of tissue solution. Final radioligand concentration was 43–48 pM. Total (1*R*)-β-CIT binding was measured at a concentration of 0.2 mg/ml, a concentration at which total binding was less than 10% of the total ligand concentration. However, a concentration of 20 mg/ml was needed to reliably measure (1*S*)-β-CIT binding and (1*R*)-β-CIT nonspecific binding. Nonspecific binding was measured by co-incubation with 1 or 10 μM (1*R*)-β-CIT. Incubation was carried out for 90 min at 22°. The assay was terminated by rapid filtration through GF/B filters on a 48-channel cell harvester (Brandel, Gaithersburg, MD). Filters were rapidly washed three times with 5 ml of ice-cold buffer and counted in a COBRA 5010 gamma counter (Packard, Meriden, CT) with an efficiency of 80%. Each determination was performed in triplicate. To reduce nonspecific filter binding, filters were pretreated with 0.05% polyethyleneimine. Binding of the radiotracer to the filter was determined by filtration of radioligand in buffer without added tissue. Tissue binding was calculated by subtracting the corresponding filter binding.

SPECT Imaging. SPECT imaging was performed in two female ovariectomized baboons with a total of 11 scanning sessions. Each baboon underwent four similar scans: two control scans with a bolus (intravenous) dose of (1*R*)-[^{123}I]β-CIT; one scan with a bolus dose of (1*S*)-[^{123}I]β-CIT; and one scan with a bolus dose of (1*S*)-[^{123}I]β-CIT followed by administration of nonradioactive (1*R*)-β-CIT (0.94 μmol/kg) at 90 min. In addition, one of the baboons was also scanned using a bolus dose of (1*R*)-[^{123}I]β-CIT followed by administration of nonradioactive (1*R*)-β-CIT at 190 min. The other baboon was scanned two additional times using a bolus plus constant infusion protocol, once with the active isomer and once with the inactive isomer. For the active isomer, the ratio of bolus to hourly infusion rate was 10 (bolus dose of 7.5 mCi (1*R*)-[^{123}I]β-CIT with an infusion rate of 0.75 mCi/hr). For the inactive isomer, the ratio of bolus to hourly infusion rate was 3 (5 mCi bolus of (1*S*)-[^{123}I]β-CIT and an infusion rate of 1.67 mCi/hr). Toward the end of this latter scan (constant infusion of (1*S*)-[^{123}I]β-CIT), at 200 min, a bolus dose of nonradioactive (1*R*)-β-CIT was given to attempt displacement of any specific binding of (1*S*)[^{123}I]-β-CIT. All administrations of nonradioactive (1*R*)-β-CIT were with a bolus dose of 0.94 μmol/kg.

Fasted animals were immobilized with ketamine (10 mg/kg intramuscularly) and then anesthetized with 2.5% isoflurane via endotracheal tube. Glycopyrrolate (10 μg/kg intramuscularly), a long-acting anticholinergic drug that does not cross the blood-brain barrier (18), was administered at the beginning of the study to decrease respiratory secretions. Vital signs were monitored every 30 min and body temperature was kept at 37° with heated water blankets. Arterial catheters were inserted for blood sampling and venous lines were inserted for administration of radiopharmaceutical and subsequent displacement drugs. Two external fiducial markers (approximately 8 mm of heat-

sealed intravenous tubing containing about 1 μCi [^{99m}Tc]$NaTcO_4$ per mCi injected dose) were glued onto each side of the head at the level of the canthomeatal line and subsequently used for uniform reorientation of the images during scan analysis. The baboon's head was immobilized in the gantry of the SPECT scanner using a bean bag that becomes rigid upon evacuation (Olympic Medical, Seattle, WA).

SPECT images were obtained with the Ceraspect camera (Digital Scintigraphics, Waltham, MA) every 3 min in control experiments with the active isomer and every 1.5 min in experiments using the inactive isomer. Images were reconstructed from photopeak counts (159 ± 16 keV) using a Butterworth filter (cutoff = 1 cm, power factor = 10) and displayed on a 64 × 64 × 32 matrix (voxel size = 3.3 × 3.3 × 3.3 mm). Attenuation correction was performed assuming uniform attenuation equal to that of water (attenuation coefficient $\mu = 0.15$ cm^{-1}) within an ellipse drawn around the brain. Using the fiducial markers, scans were reoriented in planes parallel to the canthomeatal line. The slice with the highest striatal activity was used for analysis of striatal and occipital regions. A midbrain region of interest was applied approximately four slices below this where there was minimal contamination from striatal activity. Identical regions of interest were used for all 11 scanning experiments. SPECT units of activity (cpm/voxel) were converted to μCi/ml using a conversion factor of 0.0069 μCi/cpm, determined with a 13.5-cm diameter cylindrical distributed source (19).

Peak uptake was defined as the average of the four contiguous acquisitions with the highest sum. The rate of washout was determined for regional brain activities during the 60-min period after the peak by a linear least squares fit using KaleidaGraph, version 2.1 (Synergy Software, Reading, PA). Because washout of the active isomer was so slow, the actual time at which the peak occurs was variable and highly susceptible to noise. Therefore, the time at which region of interest activity reached 95% of peak is reported here, rather than actual time to peak. Regional differences in uptake of the inactive isomer were determined from the constant infusion scan data by averaging the regional activities over the 35 min just before the time of administration of the bolus dose of nonradioactive (1*R*)-β-CIT (160–195 min after injection).

Arterial plasma concentrations of parent compound and metabolites were analyzed as described by Baldwin *et al.* (17). Briefly, arterial blood samples were drawn continuously in 20-sec intervals with a Harvard pump for 3 min, then in 1-ml aliquots at 3, 4, 6, 8, 12, 16, 20, 30, 45, and 60 min and every 30 min thereafter. Samples were stored at 0–4° until analyzed. Plasma was separated by centrifugation and aliquots were assayed in a calibrated gamma counter to measure total plasma ^{123}I radioactivity. For metabolite analysis, the plasma was extracted three times with equal volumes of ethyl acetate and the extractable activity was calculated. The organic solvent was evaporated and the residue was taken up in mobile phase and analyzed by high performance liquid chromatography. To determine protein binding, a 200-μl aliquot was subjected to centrifugal ultrafiltration with membranes having a 30,000 mol wt cutoff. The protein-bound fraction was calculated from the ratio of activity in the filter to the sum of filter and filtrate. The plasma clearance of the free parent compound (nonprotein bound) was obtained by fitting measured concentrations to a sum of three exponential functions with a weighted least squares program (Macintosh II-MATLAB version 1.2c, The Mathworks, Inc., South Natick, MA).

Results

***In vitro* homogenate binding.** The purpose of the *in vitro* studies was to compare the nonspecific binding of the ^{125}I-labeled isomers of β-CIT. The major technical difficulty was that under typical assay conditions in which total (1*R*)-[^{125}I]β-CIT binding is less than 10% of the added tracer, [^{125}I](1*R*)-β-CIT nonspecific binding and total (1*S*)-[^{125}I]β-CIT binding were extremely low. Furthermore, this low level of binding was confounded by adsorption of radiotracer to the filter, even after pretreatment of the filters with 0.05% polyethyleneimine. Under typical assay conditions, with tissue concentrations of 0.2 mg wet wt/ml buffer and a (1*R*)-[^{125}I]β-CIT concentration of approximately 45 pM, 97–99% ($n = 6$) of total caudate (1*R*)-[^{125}I]β-CIT binding was displaceable with 1 μM (1*R*)-β-CIT; of the remaining nondisplaceable binding, 56–89% was due to binding to the filter. Therefore, to better characterize the nonspecific binding, tissue concentrations of 20 mg/ml were used. At this concentration, filter binding constituted 12–56% of total inactive isomer binding or nondisplaceable active isomer binding.

The homogenate binding studies demonstrated three major findings:

1) The nonspecific binding of the active isomer was approximately equal to the total binding of the inactive isomer. Specifically, total binding of the inactive isomer in caudate (10 ± 2.9 fmol/g tissue, $n = 5$; expressed as mean ± SD for these and subsequent data) and cortex (6 ± 1.3 fmol/g tissue, $n = 6$) was approximately equal to the nonspecific binding of the active isomer in cortex (7 ± 2.7 fmol/g; $n = 6$). However, nonspecific (1*R*)-[^{125}I]β-CIT binding in caudate measured in the presence of 1 μM (1*R*)-β-CIT was 23 ± 3.5 fmol/g tissue ($n = 6$), which was higher than both total inactive isomer binding in caudate or cortex and higher than the nonspecific binding of the active isomer in cortex. At this high tissue concentration, 1 μM (1*R*)-β-CIT may not adequately block specific binding sites in the caudate. Therefore, nonspecific (1*R*)-[^{125}I]β-CIT caudate binding was also measured in the presence of 10 μM (1*R*)-β-CIT and was 4.4 ± 0.4 fmol/g tissue ($n = 3$), which was somewhat lower than total inactive isomer binding.

2) The binding of the inactive tracer was not displaceable. Total binding of (1*S*)-[^{125}I]β-CIT was 10 ± 2.9 fmol/g tissue ($n = 5$) in caudate and 6 ± 1.3 fmol/g tissue ($n = 6$) in cortex. These values were not significantly different from the binding of (1*S*)-[^{125}I]β-CIT measured in the presence of 1 μM (1*R*)-β-CIT in either caudate (10 ± 5.4 fmol/g tissue, $n = 5$) or cortex (7 ± 0.7 fmol/g tissue, $n = 5$).

3) Nonspecific binding was higher in caudate than in cortex. Total binding of the inactive isomer was 1.7-fold higher in caudate (10 ± 2.9 fmol/g tissue, $n = 5$) than in cortex (6 ± 1.3 fmol/g tissue, $n = 6$; $p = 0.02$; two-tailed, unpaired Student's t test). Similarly, nonspecific (1*R*)-[^{125}I]β-CIT binding in the presence of 10 μM (1*R*)-β-CIT was greater in caudate than cortex (4.4 ± 0.4 and 1.7 ± 0.3 fmol/g tissue, $n = 3$, respectively; $p = 0.0006$, unpaired, two-tailed Student's t test).

In vivo metabolism and SPECT imaging. The clearance of (1*R*)-[^{123}I]β-CIT (139 ± 38 liter/hr; $n = 4$) was not significantly different ($p = 0.5$, two-tailed, unpaired Student's t test) from that of (1*S*)-[^{123}I]β-CIT (121 ± 30 liter/hr; $n = 4$). Similarly, the free (non-protein-bound) fractions were the same, 25 ± 2% ($n = 4$) and 24 ± 4% ($n = 4$) for the active and inactive isomers, respectively.

The kinetics and magnitude of brain uptake of (1*S*)-[^{123}I]β-CIT in both receptor-rich (*e.g.*, striatum and midbrain) and receptor-poor (*e.g.*, occipital lobe) regions were consistent with uptake associated only with nonspecific sites (Table 1). In the striatum, the maximal uptake of the active tracer was twice that of the inactive isomer, which would be consistent with active tracer labeling DA transporters in addition to nonspecific sites. Striatal time to peak activity of the active tracer was more than 10 times longer than for the inactive tracer. The washout rate for the active isomer was only 10% of that for the

TABLE 1

SPECT scanning results summary

Peak activity, time to peak, and washout rate (mean ± SD) from scans obtained after bolus administration of (1*R*)-[^{123}I]β-CIT (n = 4) and (1*S*)-[^{123}I]β-CIT (n = 4). Tracer uptake is expressed as the regional brain activity (μCi/cm^3) divided by the injected dose (μCi) and the animal's body weight (g).

Region	Peak activity		Time to 95% of peak		Washout rate	
	Active	Inactive	Active	Inactive	Active	Inactive
	μCi/cm^3/μCi/g		min		%/hr	
Striatum	7.0 ± 1.0	3.5 ± 0.8	94 ± 41.7	12 ± 2.9	2.4 ± 3.0	26.1 ± 9.8
Occipital	3.7 ± 0.5	3.1 ± 0.7	18 ± 4.2	7 ± 1.1	31.1 ± 4.5	41.8 ± 3.7
Midbrain	4.8 ± 0.8	2.9 ± 0.7	34 ± 7.7	9 ± 2.2	11.6 ± 3.5	34.9 ± 10.6

inactive isomer, which is consistent with the significantly higher affinity of the active isomer for DA transporters. Similarly, the midbrain activity of the active isomer also peaked later and washed out more slowly than the inactive isomer, which is consistent with the high affinity of the active isomer for 5-HT transporters.

Although the occipital region is frequently used for reference as a region devoid of specific binding, there were some differences between active and inactive isomer occipital uptake (Table 1). The inactive tracer peaked earlier than the active tracer (p = 0.02, n = 4 for both active and inactive tracers) and washed out more rapidly (p = 0.01). Peak counts of the active tracer were, however, similar to that of the inactive tracer. The difference in rates may be due to the presence of a low concentration of 5-HT transporters in the cortex, as has been reported in humans by Backstrom *et al.* (20).

Similar to the homogenate-binding studies, we examined whether the uptake of the inactive tracer could be displaced, since displaceable activity is one criteria of specific binding. Following a bolus injection of (1*R*)-[^{123}I]β-CIT or (1*S*)-[^{123}I]β-CIT, a receptor-saturating dose (0.94 μmol/kg) of nonradioactive (1*R*)-β-CIT was administered at 90 min. The active radiotracer demonstrated significant displacement of both striatal and midbrain activities (Fig. 2B), whereas the inactive radiotracer showed no noticeable displacement (Fig. 2D). However, it is difficult to rule out any effect of administration of (1*R*)-β-CIT following bolus injection of (1*S*)-[^{123}I]β-CIT, as there is a significant rate of washout which is seen in the control scan also (Fig. 2C). To create a stable baseline of striatal activity, we used a protocol of bolus plus constant infusion of the radiotracer. Upon reaching equilibrium of radiotracer between plasma and brain uptake, the levels of parent tracer in blood and of brain activity would be expected to be constant. During the bolus plus constant infusion protocol shown in Fig. 3, C and D, striatal levels of (1*S*)-[^{123}I]β-CIT became relatively constant by 200 min and plasma activity by 100 min. With this stable baseline of striatal activity, injection of a pharmacological dose of nonradioactive (1*R*)-β-CIT at 190 min can be clearly seen to cause no displacement of either striatal or midbrain activities (Fig. 3C).

For the active radiotracer, equilibrium striatal binding was not achieved even after 9 hr of constant infusion (Fig. 3A). This experiment also demonstrated differences in the kinetics of striatal and midbrain activities (which reflect DA and 5-HT transporters, respectively), since striatal activity increased while midbrain activity and levels of free parent tracer in plasma decreased (Fig. 3, A and B).

Regional differences in uptake of the inactive isomer were evident in both "bolus only" and "bolus plus constant infusion"

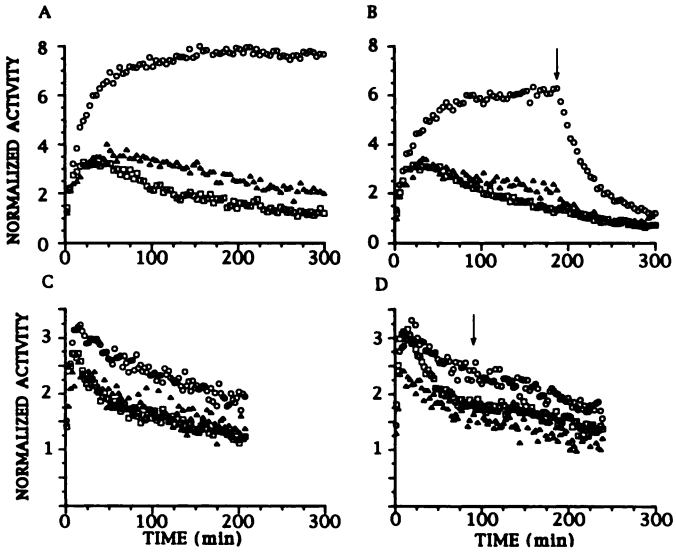

Fig. 2. Time-activity curves from the same animal after injection of (1*R*)-[^{123}I]β-CIT (A and B) and (1*S*)-[^{123}I]β-CIT (C and D). A, Bolus injection of 9.9 mCi (1*R*)-[^{123}I]β-CIT. B, Bolus injection of 5.6 mCi (1*R*)-[^{123}I]β-CIT followed by nonradioactive (1*R*)-β-CIT (0.94 μmol/kg) at 190 min (arrow). C, Bolus injection of 15.4 mCi (1*S*)-[^{123}I]β-CIT. D, Bolus injection of 15.2 mCi (1*S*)-[^{123}I]β-CIT followed by nonradioactive (1*R*)-β-CIT (0.94 μmol/kg) at 90 min (arrow). Normalized activity (μCi cm^{-3} μCi^{-1} g^{-1}) represents regional brain activity (μCi/cm^3) divided by the injected dose (μCi) and the animals body weight (g). ○, Striatum; □, occipital cortex; ▲, midbrain.

studies. Striatal activity following bolus injection of the inactive isomer was consistently higher than in the occipital lobe. Similarly, during constant infusion of the inactive tracer, striatal activity was consistently higher than that in the occipital lobe (Fig. 3C). That these differences in regional nonspecific uptake persisted under presumed equilibrium conditions demonstrated that they were not due to differences in regional blood flow.

Discussion

These studies demonstrate that (1*S*)-β-CIT provides an *in vitro* measure of nonspecific binding and an *in vivo* measure of nonspecific brain uptake. Total homogenate binding of (1*S*)-[^{125}I]β-CIT was not significantly different than the nonspecific binding of (1*R*)-[^{125}I]β-CIT. SPECT studies showed no displaceable component of (1*S*)-[^{123}I]β-CIT brain uptake. This is consistent with the findings of Wang *et al.* (16), who reported the relative affinities of the active and inactive isomers by their IC_{50} values in displacing (1*R*)-[^{125}I]β-CIT binding to rat brain homogenates. The active isomer IC_{50} reported values were 0.42 nM in striatum and 0.55 nM in cortex, while for the inactive isomer the IC_{50} reported values were 5700 nM and 450 nM, respectively.

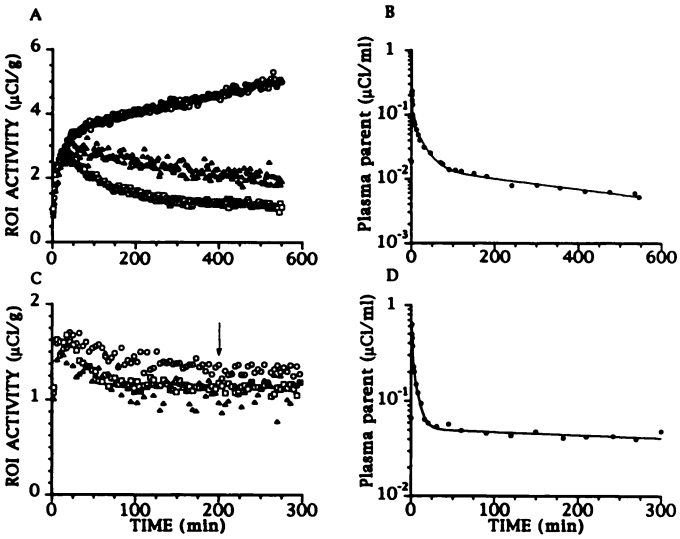

Fig. 3. Brain activity and plasma clearance curves for bolus plus constant infusion of (1*R*)-[^{123}I]β-CIT (A and B) and (1*S*)-[^{123}I]β-CIT (C and D), with both studies performed in the same animal. A & B, Regional brain uptake (A) and total plasma [^{123}I](1*R*)-β-CIT with triexponential plasma clearance curve (B). The animal received a bolus of 7.5 mCi at time 0 followed immediately by an infusion of 0.75 mCi/hr for the duration of the experiment. C & D, Regional brain uptake (C) and total plasma (1*R*)-[^{123}I]β-CIT with triexponential plasma clearance curve (D). The animal received a bolus of 5 mCi followed by an infusion of 1.67 mCi/hr for the duration of the experiment. At 200 min during the continuous infusion of (1*S*)-[^{123}I] β-CIT, a bolus dose of nonradioactive (1*R*)-β-CIT (0.94 μmol/kg) was administered (arrow). ○, Striatum; □, occipital cortex; ▲, midbrain.

Although (1*S*)-β-CIT showed no apparent specific binding, it did demonstrate regional differences in nonspecific binding in both the tissue homogenate and SPECT studies. In homogenate binding studies, the ratio of total (1*S*)-[^{125}I]β-CIT binding in caudate to that in cortex was 1.7, and in SPECT studies, brain uptake of (1*S*)-[^{123}I]β-CIT uptake was 1.2 times higher in striatum than in cortex. The smaller difference found with SPECT may be due to partial volume effects. Regional variations in nonspecific binding have been reported for several other ligands: [^{18}F]spiperone (11), [^{3}H]raclopride (12), [^{3}H](+)-cyclofoxy (15), and 3-quinuclidinyl 4-[^{125}I]iodobenzilate (21). Differences in regional nonspecific binding can introduce errors in estimates of specific binding which use ratios of regional brain activities and in compartmental models which use a region considered devoid of specific binding as an input function rather than the plasma tracer activity (12, 21, 22).

The similarity in clearances of the isomers indicates that the metabolism of β-CIT is not stereoselective, which facilitates the comparison of scan data with the two isomers. Thus, the earlier time to peak and the more rapid washout of the inactive isomer reflect the absence of (1*S*)-β-CIT specific binding and not differences in plasma levels of the isomers. The clearances of (1*R*)- and (1*S*)-β-CIT are markedly different than those reported by Gatley *et al.* (23) for the (+)- and (−)-enantiomers of cocaine. They reported that the clearance of the inactive isomer, (+)-cocaine, is 1000-fold faster than that of the naturally occurring active isomer (−)-cocaine. They suggested that this represented stereoselective hydrolysis by butyrylcholinesterase. The absence of the ester bond in β-CIT makes it a metabolically resistant cocaine analog. In addition to being nonstereoselective, the metabolism of β-CIT is significantly slower than that of (−)-cocaine (17).

Similar to other studies with stereoselective tracers (15), the transport of β-CIT across the blood-brain barrier and the kinetics of nonspecific binding would be expected to be nonstereoselective and thus identical for both isomers. Thus, the uptake of (1*S*)-[^{123}I]β-CIT should reflect the blood-brain barrier permeability and nonspecific binding kinetics of (1*R*)-[^{123}I] β-CIT. Compartmental modeling of the brain uptake of the radiolabeled inactive isomer may help to define kinetic rate constants for the active radiotracer and thereby enhance the quantitation and utility of this probe in the study of neuropsychiatric disorders.

Acknowledgments

The authors gratefully acknowledge L. Pantages-Torok, E. O. Smith, and G. Wisniewski for expert technical help.

References

1. Clarke, R. L., S. J. Daum, A. J. Gambino, M. D. Aceto, J. Pearl, M. Levitt, W. R. Cumiskey, and E. F. Bogado. Compounds affecting the central nervous system. 4. 3β-Phenyltropane-2-carboxylic acid esters and analogues. *J. Med. Chem.* **16**:1260–1267 (1973).
2. Madras, B. K., R. D. Spealman, M. A. Fahey, J. L. Neumeyer, J. K. Saha, and R. A. Milius. Cocaine receptors labeled by [^{3}H]-2β-carbomethoxy-3β-(4-fluorophenyl)tropane. *Mol. Pharmacol.* **36**:518–524 (1989).
3. Boja, J. W., A. Patel, F. I. Carroll, M. A. Rahman, A. Philip, A. H. Lewin, T. A. Kopajtic, and M. J. Kuhar. [^{125}I]RTI-55: a potent ligand for dopamine transporters. *Eur. J. Pharmacol.* **194**:133–134 (1991).
4. Neumeyer, J. L., S. Wang, R. A. Milius, R. M. Baldwin, Y. Zea-Ponce, P. B. Hoffer, E. Sybirska, M. Al-Tikriti, D. S. Charney, R. T. Malison, M. A. Laruelle, and R. B. Innis. [^{123}I]-2-β-Carbomethoxy-3-β-(4-iodophenyl)-tropane (β-CIT): high affinity SPECT radiotracer of monoamine reuptake sites in brain. *J. Med. Chem.* **34**:3144–3146 (1991).
5. Laruelle, M., R. M. Baldwin, R. T. Malison, Y. Zea-Ponce, S. S. Zoghbi, M. S. Al-Tikriti, E. H. Sybirska, R. C. Zimmermann, G. Wisniewski, J. L. Neumeyer, R. A. Milius, S. Wang, E. O. Smith, D. S. Charney, R. H. Roth, P. B. Hoffer, and R. B. Innis. SPECT imaging of dopamine and serotonin transporters with [^{123}I]CIT: pharmacological characterization of brain uptake in nonhuman primates. *Synapse* **13**:295–309 (1993).
6. Kuhar, M. J., M. C. Ritz, and J. W. Boja. The dopamine hypothesis of the reinforcing properties of cocaine. *TINS* **14**:299–302 (1991).
7. Cooper, B. R., T. J. Hester, and R. A. Maxwell. Behavioral and biochemical effects of the antidepressant bupropion (Wellbutrin): evidence for selective blockade of dopamine uptake *in vivo*. *J. Pharmacol. Exp. Ther.* **215**:127–134 (1980).
8. Kaufman, M. J., and B. K. Madras. Severe depletion of cocaine recognition sites associated with the dopamine transporter in Parkinson's diseased striatum. *Synapse* **49**:43–49 (1991).
9. Janowsky, A., F. Vocci, P. Berger, I. Angel, N. Zelnick, J. Kleinman, P. Skolnick, and S. M. Paul. [^{3}H]GBR-12935 binding to the dopamine transporter is decreased in the caudate nucleus in Parkinson's disease. *J. Neurochem.* **49**:617–621 (1987).
10. Innis, R. B., J. P. Seibyl, E. Wallace, E. Scanley, M. Laruelle, A. Abi-Dargham, Y. Zea- Ponce, S. Zoghbi, D. S. Charney, S. Wang, Y. Gao, J. L. Neumeyer, R. M. Baldwin, K. Marek, and P. B. Hoffer. SPECT imaging demonstrates loss of striatal dopamine transporters in Parkinson's disease. *J. Nucl. Med.* **34**:31P (1993).
11. Logan, J., A. P. Wolf, C.-Y. Shiue, and J. S. Fowler. Kinetic modeling of receptor-ligand binding applied to positron emission tomographic studies with neuroleptic tracers. *J. Neurochem.* **48**:73–83 (1987).
12. Seeman, P. Brain dopamine receptors in schizophrenia: PET problems. *Arch. Gen. Psychiatry* **45**:598–600 (1988).
13. Frost, J. J., K. H. Douglass, H. S. Mayberg, R. F. Dannals, J. M. Links, A. A. Wilson, H. T. Ravert, W. C. Crozier, and H. N. Wagner, Jr. Multicompartmental analysis of [^{11}C]-carfentanil binding to opiate receptors in humans measured by positron emission tomography. *J. Cereb. Blood Flow Metab.* **9**:398–409 (1989).
14. Farde, L., L. Eriksson, G. Blomquist, and C. Halldin. Kinetic analysis of central [^{11}C]-raclopride binding to D2 dopamine receptors studied with PET—a comparison to the equilibrium analysis. *J. Cereb. Blood Flow Metab.* **9**:696–708 (1989).
15. Kawai, R., Y. Sawada, M. Channing, B. Dunn, A. H. Newman, K. C. Rice, and R. G. Blasberg. Kinetic analysis of the opiate antagonist cyclofoxy in rat brain: simultaneous infusion of active and inactive enantiomers. *J. Pharmacol. Exp. Ther.* **255**:826–835 (1990).
16. Wang, S., Y. Gao, M. Laruelle, R. M. Baldwin, B. E. Scanley, R. B. Innis, and J. L. Neumeyer. Enantioselectivity of cocaine recognition sites: binding of (1*S*)- and (1*R*)-2β-carbomethoxy-3β-(4-iodophenyl)tropane (β-CIT) to monoamine transporters. *J. Med. Chem.* **36**:1914–1917 (1993).
17. Baldwin, R. M., Y. Zea-Ponce, S. S. Zoghbi, M. Laruelle, M. S. Al-Tikriti, E. H. Sybirska, R. T. Malison, J. L. Neumeyer, R. A. Milius, S. Wang, M.

Stabin, E. O. Smith, D. S. Charney, P. B. Hoffer, and R. B. Innis. Evaluation of the monoamine uptake site ligand [^{123}I] methyl 3β-(4-iodophenyl)-tropane-2β-carboxylate ([^{123}I]β-CIT) in non-human primates: pharmacokinetics, biodistribution, and SPECT brain imaging coregistered with MRI. *Nucl. Med. Biol.* **20**:597–606 (1993).

18. Proakis, A. G., and G. B. Harris. Comparative penetration of glycopyrolate and atropine across the blood-brain and placental barriers in anesthetized dogs. *Anesthesiology* **48**:339–344 (1978).
19. Laruelle, M., A. Abi-Dargham, Z. Rattner, M. S. Al-Tikriti, Y. Zea-Ponce, S. S. Zoghbi, D. S. Charney, J. Price, J. J. Frost, P. B. Hoffer, R. M. Baldwin, and R. B. Innis. Single photon emission tomography measurement of benzodiazepine receptor number and affinity in primate brain: a constant infusion paradigm with [^{123}I]iomazenil. *Eur. J. Pharmacol.* **230**:119–123 (1993).
20. Backstrom, I., M. Bergstrom, and J. Marcusson. High affinity [^{3}H]paroxetine binding to serotonin uptake sites in human brain. *Brain Res.* **486**:261 (1989).
21. Sawada, Y., S. Hiraga, B. Francis, C. Patlak, K. Pettigrew, K. Ito, E. Owens, R. Gibson, R. Reba, W. Eckelman, S. Larson, and R. G. Blasberg. Kinetic analysis of 3-quinuclididinyl 4-[^{125}I]iodobenzilate transport and specific binding to muscarinic acetylcholine receptor in rat brain *in vivo*: implications for human studies. *J. Cereb. Blood Flow Metab.* **10**:781–807 (1990).
22. Kawai, R., R. E. Carson, B. Dunn, A. H. Newman, K. C. Rice, and R. G. Blasberg. Regional brain measurement of B_{max} and K_D with the opiate antagonist cyclofoxy: equilibrium studies in the conscious rat. *J. Cereb. Blood Flow Metab.* **11**:529–544 (1991).
23. Gatley, S. J., R. R. MacGregor, J. S. Fowler, A. P. Wolf, S. L. Dewey, and D. J. Schlyer. Rapid stereoselective hydrolysis of (+)-cocaine in baboon plasma prevents its uptake in the brain: implications for behavioral studies. *J. Neurochem.* **54**:720–723 (1990).

Send reprint requests to: B.E. Scanley, M.D., Ph.D., VA Medical Center/116A2, 950 Campbell Avenue, West Haven, CT 06516.